Cell PRESS
Cell Stem Cell
Article

Pbx1 Regulates Self-Renewal of Long-Term Hematopoietic Stem Cells by Maintaining Their Quiescence

Francesca Ficara,[1] Mark J. Murphy,[1] Min Lin,[1] and Michael L. Cleary[1,*]
[1]Department of Pathology, Stanford University School of Medicine, Stanford, CA 94305, USA
*Correspondence: mcleary@stanford.edu
DOI 10.1016/j.stem.2008.03.004

SUMMARY

Self-renewal is a defining characteristic of stem cells; however, the molecular pathways underlying its regulation are poorly understood. Here, we demonstrate that conditional inactivation of the *Pbx1* proto-oncogene in the hematopoietic compartment results in a progressive loss of long-term hematopoietic stem cells (LT-HSCs) that is associated with concomitant reduction in their quiescence, leading to a defect in the maintenance of self-renewal as assessed by serial transplantation. Transcriptional profiling revealed that multiple stem cell maintenance factors are perturbed in *Pbx1*-deficient LT-HSCs, which prematurely express a large subset of genes, including cell-cycle regulators, normally expressed in non-self-renewing multipotent progenitors. A significant proportion of Pbx1-dependent genes is associated with the TGF-β pathway, which serves a major role in maintaining HSC quiescence. Prospectively isolated, *Pbx1*-deficient LT-HSCs display altered transcriptional responses to TGF-β stimulation in vitro, suggesting a possible mechanism through which Pbx1 maintenance of stem cell quiescence may in part be achieved.

INTRODUCTION

Hematopoietic stem cells (HSCs) are distinguished by their inherent capacity to self-renew and differentiate into multiple blood cell lineages throughout the life of the host. These crucial defining attributes of HSCs must be tightly regulated and intricately balanced in order to maintain homeostasis of the lympho-hematopoietic system and to prevent the emergence of blood cell malignancies.

A number of molecules have been implicated in the regulation of HSC self-renewal, including cell-intrinsic transcription factors (Tel/Etv6, Gfi1, HoxB4, c-Myc, Zfx, and FoxO1/3/4), signal transducers (Pten), and epigenetic regulators (Bmi-1 and Ezh2), as well as extrinsic (niche-induced) factors, such as Tek/Angpt1 and TGF-β signaling (Akala and Clarke, 2006; Galan-Caridad et al., 2007; Kamminga et al., 2006; Tothova et al., 2007). HSCs may also undergo various fates that prevent further self-renewal, including differentiation into more committed progenitor cells (inhibited by HoxB4, promoted by c-Myc), apoptosis (inhibited by Zfx and FoxO), or senescence (inhibited by Bmi1) (reviewed by Cellot and Sauvageau, 2007). To maintain a steady-state pool of self-renewing cells and prevent exhaustion, HSCs must limit their cell divisions and return to G_0 until the next self-renewing cycle is required. At any one time, only a small proportion of the LT-HSC population is actually in cycle (Venezia et al., 2004), and regulation of the ability to enter and exit quiescence is the most critical requirement for long-term maintenance of the stem cell pool.

Pbx1 is a TALE class homeodomain transcription factor that critically regulates numerous embryonic processes, including morphologic patterning, organogenesis, and hematopoiesis (DiMartino et al., 2001; Kim et al., 2002; Manley et al., 2004; Schnabel et al., 2003a, 2003b; Selleri et al., 2001). It is a component of hetero-oligomeric protein complexes that regulate developmental gene expression in part through modulation of Hox protein DNA-binding and context-dependent transcriptional effector functions (Saleh et al., 2000). As a complex with other TALE class proteins, Pbx1 may mark specific genes for activation by penetration of repressive chromatin and recruitment of coactivators (Berkes et al., 2004). As a major global developmental regulator, Pbx1 has been implicated in promoting progenitor cell proliferation in multiple tissues (Moens and Selleri, 2006). Its function in adult tissue stem cells, however, is unknown, although a potential role is suggested by the observation that Pbx1 is preferentially expressed in LT-HSCs compared to more mature ST-HSCs and multipotent progenitor cells (MPPs) in the hematopoietic system (Forsberg et al., 2005; Kiel et al., 2005).

In this report, we employed a genetic approach to conditionally inactivate Pbx1 in the mouse hematopoietic system in vivo. In contrast to its role in promoting progenitor expansion, we report that Pbx1 positively regulates HSC quiescence. Our studies demonstrate that Pbx1 is a regulator of HSC self-renewal that contributes to maintenance of HSC quiescence through multiple pathways, including the transcriptional program induced in response to TGF-β signaling.

RESULTS

Postnatal Hematopoiesis Is Perturbed in the Absence of Pbx1

Pbx1-conditional knockout (KO) mice were employed to study the role of Pbx1 in the mouse adult hematopoietic system

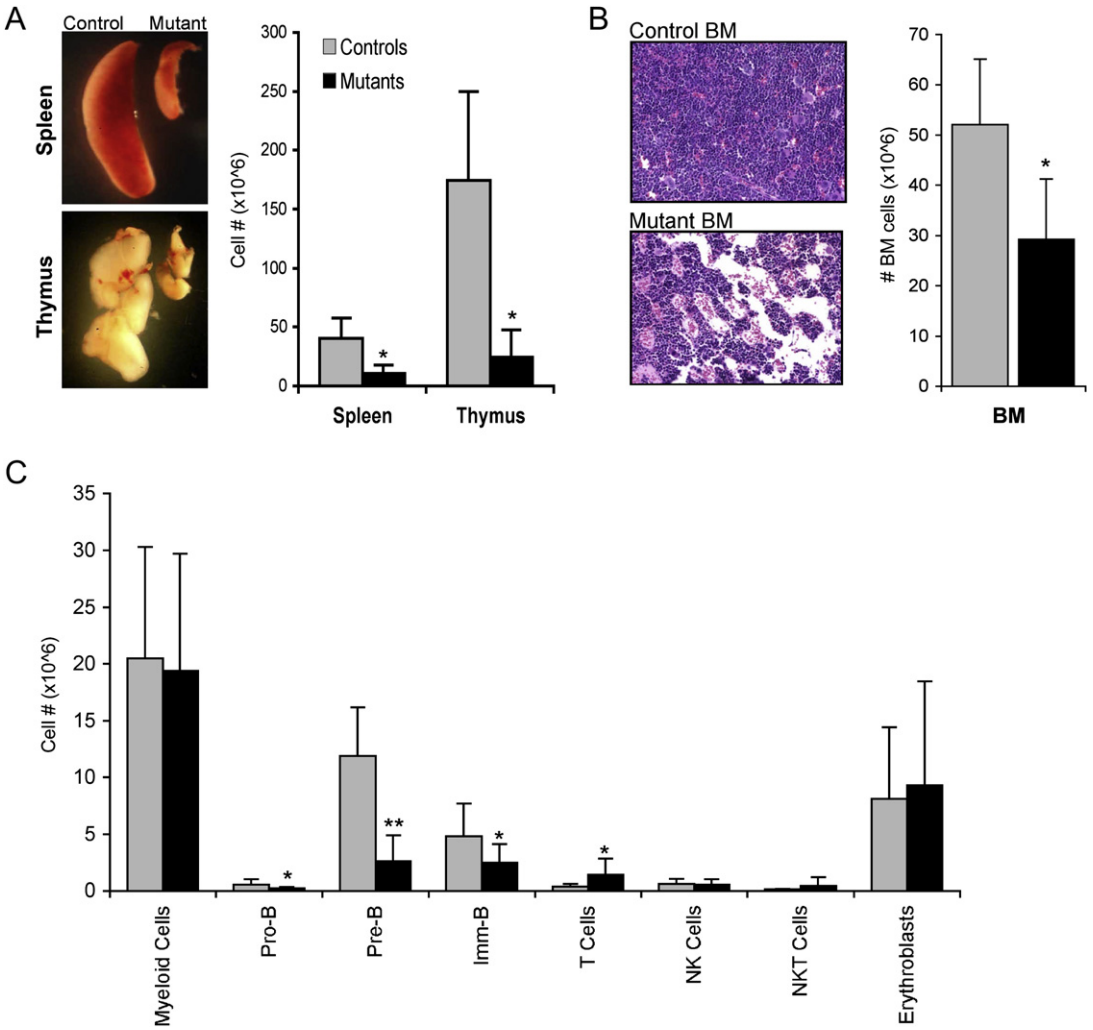

Figure 1. Hematopoietic Defects in Pbx1-Conditional KO Mice

(A) Gross appearance is shown for spleen (top left) and thymus (bottom left) of 5-week-old representative *Tie2Cre*$^{+}$.*Pbx1*$^{+/f}$ control and *Tie2Cre*$^{+}$.*Pbx1*$^{-/f}$ mutant mice. Histograms on the right show the average number (±SD) of hematopoietic cells in the respective organs (*p < 0.00001, n = 14 and 27 for spleen and thymus, respectively).

(B) Hypocellular BM in mutant mice is revealed by H&E staining of decalcified BM sections from 6-week-old mice. Histogram on the right shows average BM cell counts as total nucleated blood cells in femurs and tibiae. Controls are *Tie2Cre*$^{+}$.*Pbx1*$^{+/f}$ (*p = 0.005, n = 7).

(C) Histogram represents cell numbers for the indicated populations as determined by FACS analysis on BM of 3- to 4-week-old mice. Myeloid cells, CD11b^{+}; ProB cells, B220^{+}CD43^{+}IgM^{-}; PreB cells, B220^{+}CD43^{-}IgM^{-}; immature B cells (ImmB), B220^{+}CD43^{-}IgM^{+}; T cells, TCRβ^{+}; NK cells, TCRβ^{-}NK1.1^{+}; and NKT cells, TCRβ^{+}NK1.1^{+} (*p < 0.03; **p < 0.00004, n = 11).

(Figure S1A available online). Homozygous *Pbx1* floxed mice (*Pbx1*$^{f/f}$) were crossed with *Pbx1*$^{+/-}$ mice (Selleri et al., 2001) expressing Cre under the control of the *Tie2* promoter (*Tie2Cre*$^{+}$.*Pbx1*$^{+/-}$ mice), which specifically drives Cre expression in endothelial cells and HSCs (Chang et al., 2004; Kisanuki et al., 2001). PCR analysis of the resulting *Tie2Cre*$^{+}$.*Pbx1*$^{-/f}$ mice (referred to hereafter as "mutant" mice) showed specific and complete deletion of *Pbx1* in different hematopoietic tissues, including peripheral blood (PB), bone marrow (BM), spleen, thymus, and lymph nodes (Figure S1B), as expected from efficient excision of *Pbx1* in HSCs.

The hematopoietic organs appeared normal at birth, indicating proper embryonic development, but displayed major defects in young mutant mice. The thymus and spleen were dramatically reduced in size and showed pronounced histologic disorganization (Figure 1A and data not shown) compared to controls (*Tie2Cre*$^{+}$.*Pbx1*$^{+/f}$, *Tie2Cre*$^{-}$.*Pbx1*$^{+/f}$, or *Tie2Cre*$^{-}$.*Pbx1*$^{-/f}$ mice, which did not differ in any of the phenotypes to be described and, hence, will not be further distinguished). Differences in the absolute numbers of CD45^{+} cells between mutant mice and controls (4-fold and 7-fold in spleen and thymus, respectively) indicated that the reduced organ sizes were mainly due to a lower content of hematopoietic cells (Figure 1A). In the thymus, FACS analysis showed that all T-lineage cellular subpopulations were reduced, starting from the most immature DN1 stage (data not shown), suggesting that the defect arose at a very early stage of T-lymphocyte development. The BM of mutant mice compared to controls was hypocellular (Figure 1B), mainly accounted

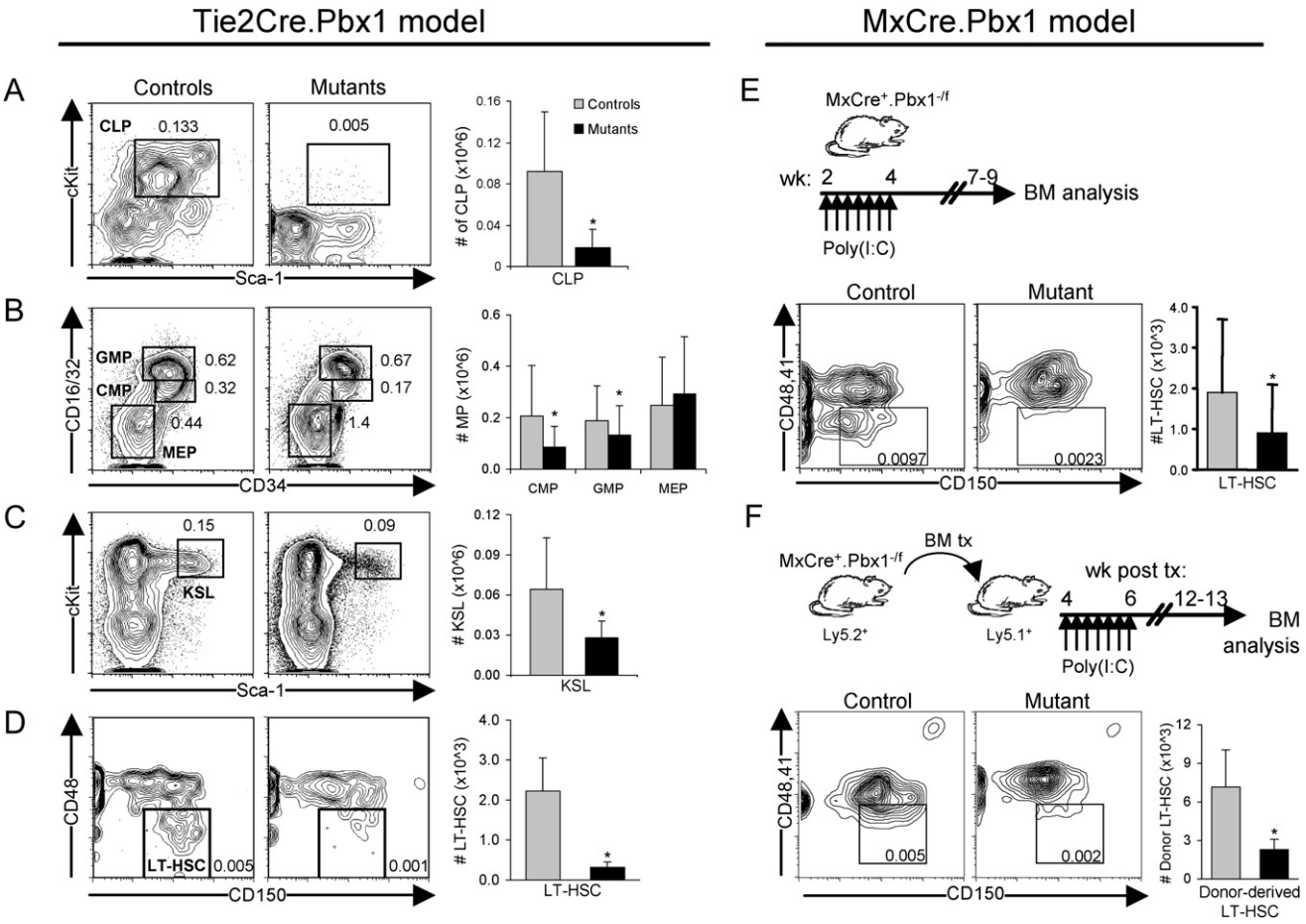

Figure 2. Decreased BM Stem and Progenitor Cells in Pbx1 Mutant Mice

(A–D) Representative FACS analyses (left) and average absolute numbers (right) of BM cells are shown for control *Tie2Cre*$^{+}$*.Pbx1*$^{+/f}$ and mutant *Tie2Cre*$^{+}$*.Pbx1*$^{-/f}$ mice. Numbers in the FACS plots indicate percentages among total BM cells.

(A) CLPs are defined as Lin^{-}IL7R^{+}Sca1^{lo}cKit^{lo} (Kondo et al., 1997). Depicted contour plots are referred to the Lin^{-}IL7R^{+} gate (*p < 0.02, n = 5).

(B) FACS plots are referred to the Lin^{-}cKit^{hi}Sca1^{-} gate, in which CMPs are defined as CD34$^{+/lo}$CD16/32^{int}, GMPs as CD34^{+}CD16/32^{+}, and MEPs as CD34^{-}CD16/32^{-} (*p < 0.005, n = 17).

(C) KSL cells are Lin^{-}IL7R^{-}Sca1^{+}cKit^{+} (*p < 0.03, n = 7).

(D) LT-HSCs are defined as KSL, CD150^{+}CD41^{-}CD48^{-}. FACS plots are referred to the KSL gate (*p < 0.0001, n = 10).

(E and F) Experimental outline, representative FACS analyses, and average absolute numbers of LT-HSCs in control and *MxCre*$^{+}$*.Pbx1*$^{-/f}$ mice. Indicated mice received seven poly(I:C) injections every other day. FACS plots are referred to the KSL gate, percentages among total BM cells are indicated (*p = 0.02, n = 24). In (F), 1 × 10^{6} donor cells either from mutant or control (*MxCre*$^{-}$*.Pbx1*$^{f/f}$) mice were transplanted into lethally irradiated Ly5.1 recipients prior to poly(I:C) injections. KSL cells were all donor derived (*p = 0.01, n = 4).

for by decreased B-lineage cells as revealed by FACS analysis (Figure 1C). The reduction in the B cell compartment was highly significant starting from the pro-B (B220^{+}CD43^{+}IgM^{-}) cell stage with pre-B (B220^{+}CD43^{-}IgM^{-}) cells constituting the population numerically most reduced. Thus, Pbx1 is necessary to maintain the postnatal hematopoietic compartment.

Lack of Pbx1 Impairs the Maintenance of Stem and Progenitor Cells through Loss of Quiescence

FACS analyses revealed marked reduction of common lymphoid progenitors (CLPs) (Figure 2A and Figure S2A), mild reductions in the total numbers of common myeloid progenitors (CMPs, Figure 2B) and to a lesser extent of granulocyte-monocyte progenitors (GMPs), and reduced frequency of colony-forming cells in semisolid culture (CFCs, Figure S2B). More importantly, there was a marked reduction of the HSC-enriched Lin^{-}c-Kit^{+}Sca-1^{+} (KSL) cell population (Figure 2C). Analysis of the LT-HSCs within this population (Kiel et al., 2005) revealed a considerable reduction in their numbers, indicating a defect at the earliest stage of adult hematopoietic development (Figure 2D), suggesting that the reduction of different progenitor cell populations predominantly originated from a reduced number of LT-HSCs. The described stem and progenitor abnormalities were progressive as the mice aged, being undetectable at birth (Figure S2C), variable at 2 weeks of age (in three out of five mutants analyzed), and prominent from 3 weeks of age onward.

To rule out the possibility that a vascular niche defect to which HSCs were exposed during development could be responsible for the observed hematopoietic abnormalities, *Pbx1*$^{f/f}$ mice were crossed with *MxCre*$^{+}$*.Pbx1*$^{+/-}$ mice. Highly efficient *Pbx1*

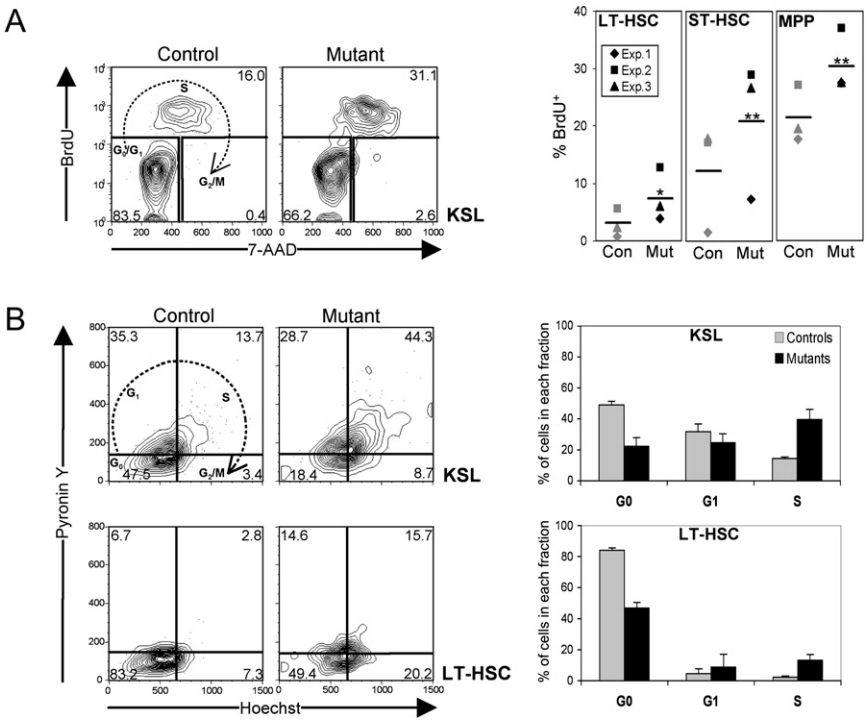

Figure 3. *Pbx1*-Deficient Stem Cells Display Increased Cycling and Reduced Quiescence

(A) Control or mutant mice were injected i.p. with BrdU and sacrificed 2 hr later. Representative FACS analyses on the left show BrdU and 7-AAD incorporation in KSL cells. Graphs on the right represent the percentage of $BrdU^+$ cells in LT-HSCs, ST-HSCs, and MPP cells in three independent experiments (*p = 0.06, **p < 0.04).

(B) Left, representative FACS analysis of PY/Hoechst staining on KSL cells (top) or LT-HSCs (bottom). Right, percentage of KSL cells (top) or LT-HSCs (bottom) in G_0, G_1, and S phase (n = 2, with bars representing the range).

deletion was induced with poly(I:C) in young *MxCre*$^+$.*Pbx1*$^{f/f}$ (or $^{-/f}$) mutant mice and confirmed by qRT-PCR 3 to 4 weeks later (Figure S3A). Defects in the stem cell compartment of *MxCre*$^+$.*Pbx1*$^{f/f}$ (or $^{-/f}$) mice were identical to those observed with *Tie2Cre*$^+$.*Pbx1*$^{-/f}$ mice (Figure 2E and Figure S3B), and similar defects were also observed in CLPs, CMPs, and B cells (Figures S3C and S3D and data not shown). To further exclude a primary BM microenvironmental cause underlying the HSC defect, BM cells from *MxCre*$^+$.*Pbx1*$^{f/f}$ mice were transplanted into wild-type (WT) recipients, and deletion of *Pbx1* in donor cells was induced with poly(I:C) after BM reconstitution. LT-HSCs were reduced as a result of *Pbx1* excision exclusively in the hematopoietic compartment (Figure 2F). Furthermore, transplant of WT BM cells into *MxCre*$^+$.*Pbx1*$^{f/f}$ (or $^{-/f}$) mice (Figure S3E) showed that donor-derived HSCs were not reduced upon induction of *Pbx1* deletion in mutant recipient mice, unequivocally demonstrating that the absence of Pbx1 from a nonhematopoietic compartment does not contribute to the HSC phenotype.

The underlying cause for reduced numbers of *Pbx1* null stem and progenitor cells was not a consequence of increased levels of in vivo apoptosis, because Annexin V staining did not reveal increased retention in KSL cells (data not shown), LT-HSCs (Figure S2D), or in myeloid or lymphoid progenitors (data not shown) from mutant mice. Conversely, assessment of cellular proliferation by BrdU pulse labeling experiments revealed significantly higher BrdU incorporation in all KSL cell subpopulations, starting from LT-HSCs (Figure 3A). A more detailed analysis of the cell cycle by Hoechst/Pyronin Y staining revealed that far fewer mutant KSL and LT-HSCs were in the G_0 phase, with a much higher proportion in SG_2M (Figure 3B). These data suggested that increased proliferation likely contributes to the reduced numbers of LT-HSCs by diminishing the pool of quiescent stem cells.

Pbx1-Deficient HSCs Display Intrinsic Functional Defects and Impaired Long-Term Engraftment

In competitive repopulation assays, escalating doses of total BM cells from mutant or control mice (Ly5.2) were infused into lethally irradiated congenic recipients (Ly5.1), in competition with a fixed number of BM cells from Ly5.1/Ly5.2 mice. FACS analysis of blood leukocytes from transplanted animals revealed that BM cells from mutant mice were completely unable to compete with WT cells even when transplanted at a 10-fold higher dose of mutant cells than competitor cells (Figure 4A). Donor *Tie2Cre*$^+$.*Pbx1*$^{-/f}$ cells were undetectable also in the BM (data not shown). The inability to compete with WT BM was not simply due to a lower content of mutant stem cells, because the same number of total BM cells from mutant or control mice were transplanted, and the difference in the proportion of KSL and of LT-HSCs was much less than 10-fold (Figures 2C and 2D, FACS plots). These data demonstrate a profound functional impairment of LT-HSCs in the absence of Pbx1.

To assess if *Pbx1*-deficient stem cells are intrinsically capable of engraftment and/or differentiation, different doses of BM cells from mutant or control mice were infused into lethally irradiated recipients in the absence of competitor cells. Analysis of PB for cells of donor origin after transplant showed that, in the absence of competition, efficient engraftment by *Pbx1* null BM cells was achieved, but only at high transplanted cell doses (Figure 4B; only myeloid cell data are shown for simplicity, because their high turnover provides a good measure of stem cell activity). At lower cell doses (2×10^5 or less total BM cells), engraftment was mostly short term (middle and right panels) and less efficient (right panel), in accordance with an insufficient number of functional HSCs transplanted from mutant mice. Once engrafted, multilineage differentiation was achieved (Figure S4), confirming that differentiation and migration were not abrogated by lack of Pbx1. PCR performed on genomic DNA isolated from donor blood leukocytes several weeks posttransplant confirmed complete excision of the floxed *Pbx1* allele (Figure 4C), demonstrating that reconstitution was not mediated by rare undeleted cells present in the BM of conditional KO mice prior to transplant. Thus, Pbx1 null HSCs can engraft, differentiate, and reconstitute

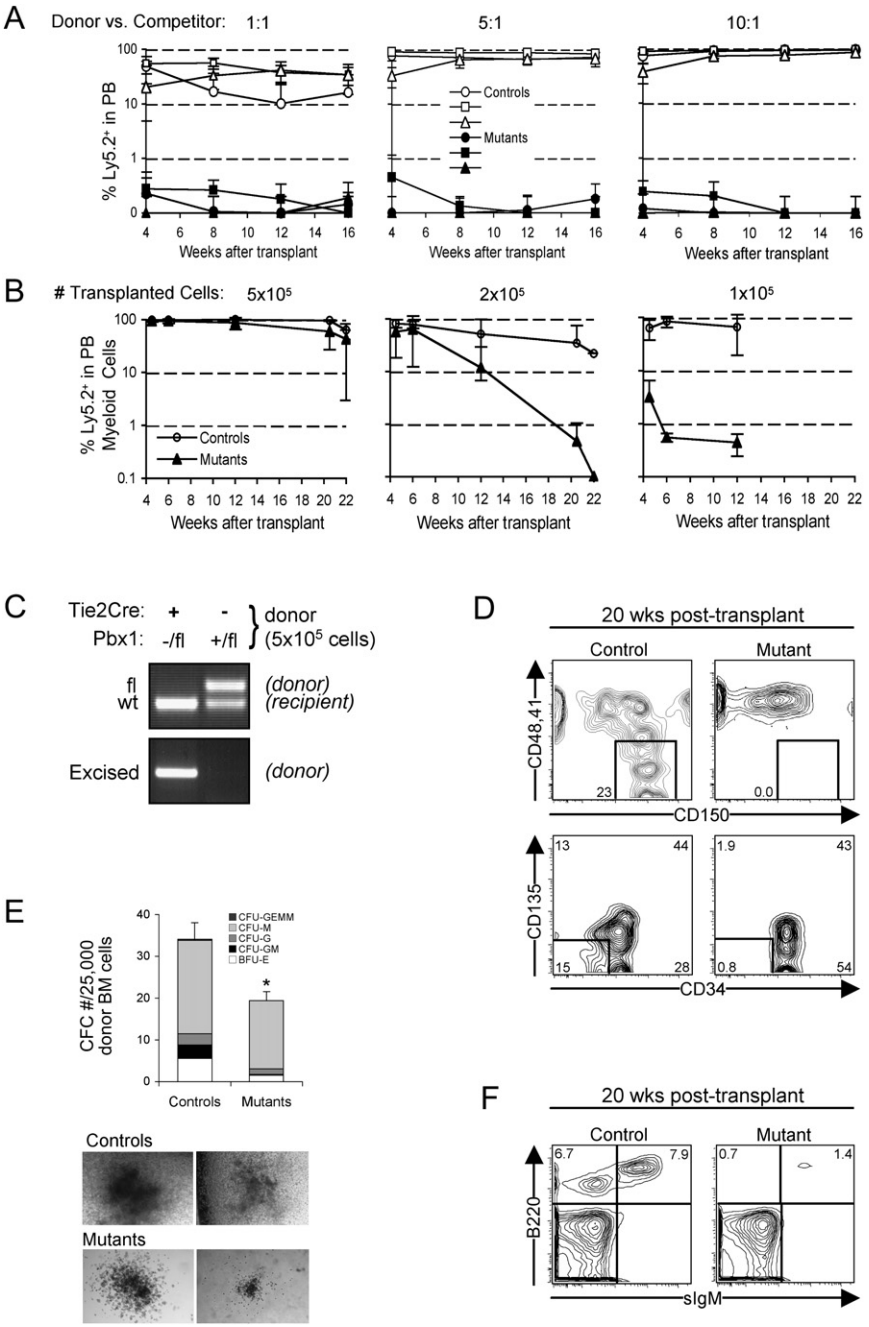

Figure 4. Defective Stem Cell Function in Pbx1 Mutant Mice

(A) Total BM cells from either control (white) or mutant (black) Ly5.2 mice were transplanted into lethally irradiated Ly5.1 recipients in competition with BM from Ly5.1/Ly5.2 mice, at different ratios of donor versus competitor, as indicated at the top of the panels. The average percentages of myeloid (circles), B (squares), and T (triangles) cells of donor origin in the PB of recipient mice are shown for different time points after transplant. The percentages of Ly5.2$^+$ cells were measured by FACS in the CD11b$^+$, B220$^+$, and TCRβ^+ fractions of red blood cell (RBC)-lysed PB. The data are from two independent experiments (four to five recipients/group).

(B) Different doses of total BM cells (indicated at top of panels) from either control or mutant Ly5.2 mice were transplanted into lethally irradiated Ly5.1 recipients in the absence of competition. The percentage of donor myeloid cells in the PB of recipient mice was determined at different time points after transplant.

(C) Representative PCR performed on the PB of recipients of noncompetitive transplants shows that reconstitution was mediated by cells with complete Pbx1 deletion in mice transplanted with mutant BM.

(D) Representative FACS analyses are shown for HSCs at week 20 posttransplant of 5 × 10^5 donor whole BM cells with two different combinations of antibodies. Top panels, LT-HSCs are defined as KSL,CD150$^+$CD48$^-$; bottom panels, LT-HSCs are defined as KSL,CD34$^-$CD135$^-$ (Mansson et al., 2007; Rossi et al., 2005). Plots and percentages are referred to the donor KSL gate.

(E) Methylcellulose colony assays were performed at the time of sacrifice 20 weeks posttransplant with BM cells of donor origin from mice that received noncompetitive transplants.

(F) Representative FACS analyses are shown for B cells of donor origin (Ly5.2 gate) in the BM at week 20 after noncompetitive transplantation.

hematopoiesis in lethally irradiated recipients, but only under noncompetitive conditions.

Despite engraftment by *Pbx1*-deficient cells, progressive graft failure was observed long term after transplant (>20 weeks, Figure 4B), in accordance with a defect at the level of LT-HSCs. Indeed, 20 weeks after transplant with 5 × 10^5 *Pbx1* null BM cells, phenotypically defined LT-HSCs were below the limit of detection in the BM of recipient mice (Figure 4D). Accordingly, in methylcellulose in vitro colony assays performed at the same time point, CFU-GEMM colonies were not detected after plating of FACS-sorted (Ly5.1) donor BM cells from mice transplanted with *Pbx1* null cells (Figure 4E, top) nor were any colonies derived from high proliferative potential progenitors (Figure 4E, bottom). Moreover, similar to the BM of mutant mice prior to transplant (Figure S2), the number of total colonies obtained was significantly reduced, mainly due to a decreased number of BFU-E and CFU-GM, indicating a defect at the level of progenitors in addition to LT-HSCs, as predicted by the lower proportion and absolute number of CMP in the conditional KO mice (Figure 2B). In the BM of recipients transplanted with cells from *Pbx1* mutants, the proportion of B cells derived from the donor was also considerably lower (Figure 4F). Due to their advanced age at the time of analysis, transplanted mice exhibited small thymi and a very low proportion of CLPs independent of the genotypes of the donor mice. However, a reduced proportion of B cells in the BM (but not in the blood) was in accordance with a progressive CLP or early B cell progenitor defect. Hence, most of the features of the conditional KO mice (low numbers of stem, progenitor, and B cells in

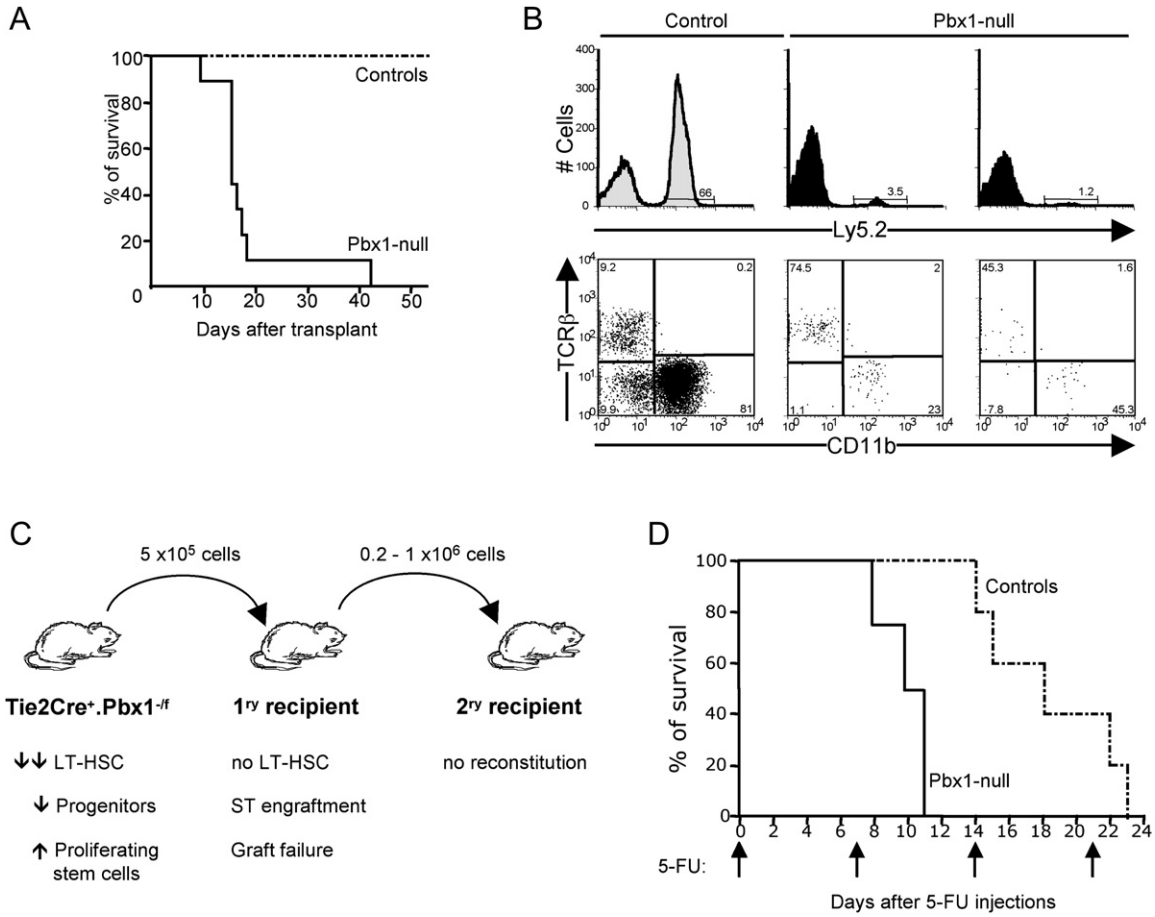

Figure 5. Pbx1-Deficient Cells Do Not Engraft Secondary Recipients

(A) Survival curves represent results of secondary transplants performed with donor BM cells sorted from primary recipient mice (20 weeks after primary transplant) successfully reconstituted by control or mutant cells. Data are derived from two independent experiments containing a total of nine secondary transplanted mice in each cohort.

(B) Representative FACS analysis of PB at 4 weeks posttransplant is shown for secondary recipients transplanted with control (left) or mutant (right, two examples) BM cells. Top, percentage of donor cells; bottom, percentage of myeloid and T cells in the donor gate. Double-negative cells are $B220^+$ B cells (data not shown).

(C) Summary of transplantation experiments.

(D) Survival curves after multiple 5-FU injections (indicated by arrows) of poly(I:C)-treated mutant (*MxCre*$^+$.*Pbx1*$^{-/f}$ or *MxCre*$^+$.*Pbx1*$^{f/f}$, n = 4) and control (*MxCre*$^-$.*Pbx1*$^{f/f}$, *MxCre*$^-$.*Pbx1*$^{-/f}$, or *MxCre*$^-$.*Pbx1*$^{+/f}$, n = 5) mice.

the BM) were reproduced in the transplanted mice and thus constitute intrinsic stem and progenitor cell defects.

Pbx1-Deficient LT-HSCs Are Unable to Self-Renew

The progressive graft failure and exhaustion of mutant LT-HSCs (KSL, $CD150^+CD48^-CD41^-$ or KSL, $CD34^-CD135^-$ cells) in the primary transplant recipients (Figure 4D) suggested a defect in self-renewal. Therefore, secondary transplant experiments were performed to confirm the reduction of functional Pbx1 null LT-HSCs in the BM of primary transplant recipients. Twenty weeks after primary transplant, total BM cells from mice noncompetitively reconstituted with 5×10^5 BM cells/mouse were harvested and sorted according to the donor Ly5.1 marker. Sorted donor cells were then transplanted into secondary recipients at escalating doses without competitor cells. *Pbx1*-deficient cells were unable to engraft secondary recipients (Figure 5A). Analysis of the blood of secondary recipients before death revealed low but detectable chimerism (Figure 5B), indicating that the few HSCs originally derived from mutant mice homed in the BM of secondary recipients but failed to fully reconstitute. Therefore, phenotypic and functional LT-HSCs rapidly declined to undetectable levels after sequential transplants of BM cells from mutant mice to primary and secondary recipients (summarized in Figure 5C).

Hematopoietic reconstitution was also assessed in situ in primary mutant mice by monitoring survival upon sequential injections of the cell-cycle-dependent myelotoxic agent 5-fluorouracil (5-FU) (Cheng et al., 2000), an assay that does not depend on engraftment. The requirement for a relatively long follow-up prompted the use of the MxCre conditional KO model, because *Tie2Cre*$^+$.*Pbx1*$^{-/f}$ mice have a short life span. Five weeks after the last poly(I:C) injection, mutant and control mice

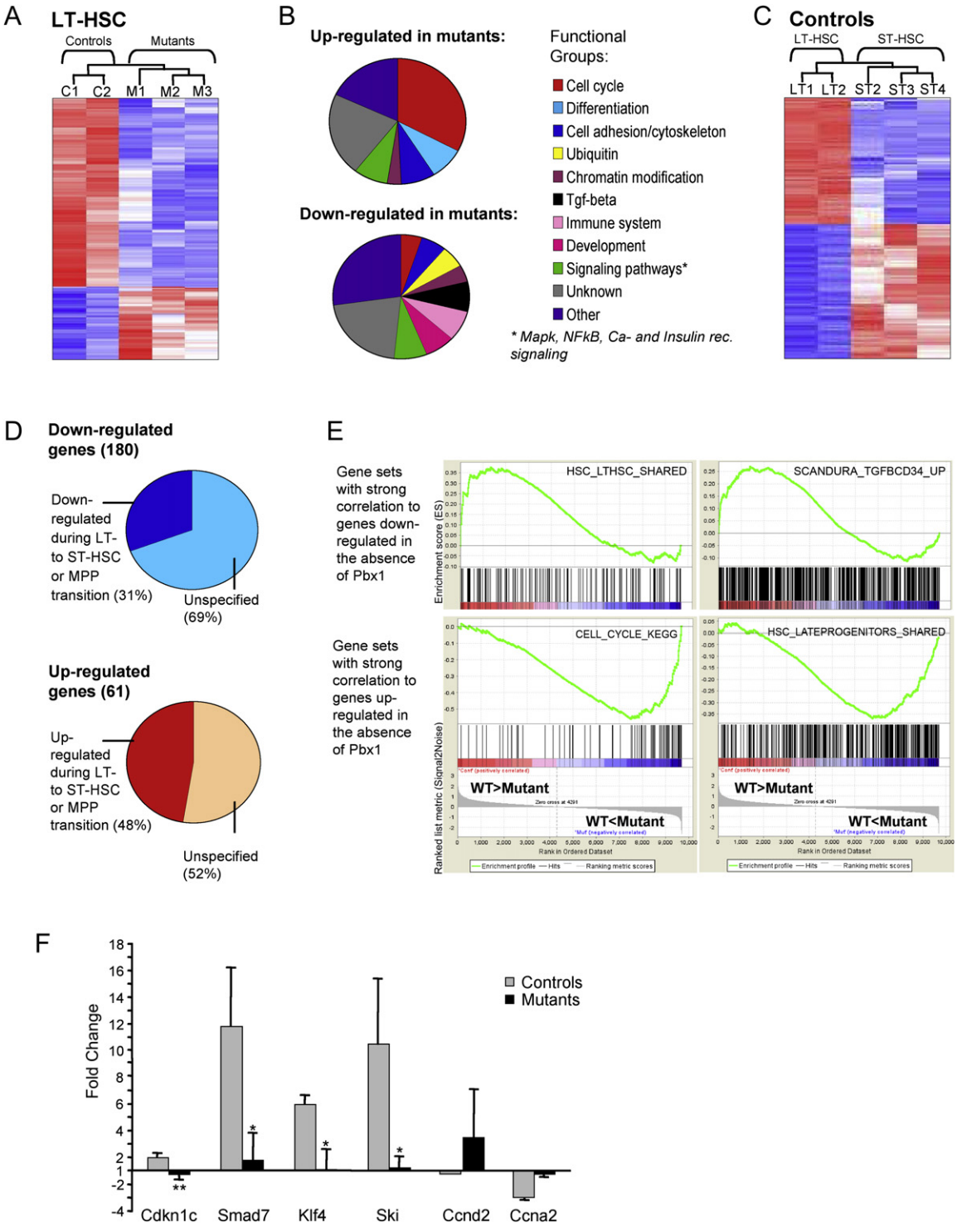

Figure 6. Gene Expression Profile of Pbx1-Deficient HSCs

(A) Heat map shows the expression of the 241 Pbx1-regulated genes in LT-HSCs from poly(I:C)-treated control (*MxCre*$^{-}$.*Pbx1*$^{f/f}$, C1, and C2) or mutant (*MxCre*$^{+}$.*Pbx1*$^{f/f}$, M1–M3) individual mice. Upregulated and downregulated genes are presented in red and blue, respectively.

(B) Pie charts show the distribution of the 61 upregulated (top) and the 180 downregulated (bottom) genes in Pbx1-deficient LT-HSCs into functional groups.

(C) Heat map displays the differentially expressed transcripts in LT- and ST-HSCs from poly(I:C)-treated control mice.

(D) Pie charts represent the overlap of the mutant LT-HSC gene signature with genes found in the current study to be differentially expressed in the LT- to ST-HSC transition in control mice (17% and 37% for the downregulated and upregulated genes, respectively), as well as with genes differentially expressed in the LT-HSC to MPP transition not included in the LT/ST-HSC overlap (14% and 11%).

received 5-FU at 7 day intervals to kill proliferating cells, including hematopoietic progenitors, thus providing a stimulus for HSCs to proliferate in order to replenish the hematopoietic system. *Pbx1*-deficient mice succumbed after the second 5-FU injection, whereas exhaustion of the HSC pool occurred significantly later in control mice (Figure 5D). Mutant mice died of hematopoietic failure, with pancytopenia in the blood and BM (data not shown).

Taken together, our data demonstrate that Pbx1 maintains the hematopoietic system by regulating LT-HSC self-renewal.

A Pbx1-Dependent Transcriptional Program Implicates Perturbation of Multiple Pathways in Loss of LT-HSC Quiescence and Self-Renewal

Global gene expression profiling analyses were performed to identify Pbx1-dependent genes and pathways involved in the regulation of HSC self-renewal. For these studies, *Pbx1* deletion was induced in *MxCre*$^{+}$.*Pbx1*$^{f/f}$ mutant mice, which allowed the use of older animals to obtain a much higher yield of LT-HSCs and also the distinction between LT- and ST-HSCs in adult mice based on the expression of CD34 and CD135 markers in KSL cells. Cells were prospectively sorted from BM harvested 4 weeks after the last injection of poly(I:C).

Analysis of gene expression data from mutant and control LT-HSCs revealed 241 nonredundant differentially expressed genes, of which 61 were upregulated and 180 downregulated in *Pbx1* mutants (Figure 6A and Table S1). Microarray results were confirmed by qRT-PCR for a small subset of the genes (Table S1). Classification based on functional annotation revealed that a large proportion of upregulated genes in *Pbx1* mutant LT-HSCs belonged to cell-cycle ontogeny groups (Figure 6B), consistent with the observed increase in cycling stem cells leading to loss of their self-renewal potential. Notably, ~8% of the downregulated genes belonged to the TGF-β signaling pathway (Figure 6B and Table S2), which has been previously implicated in maintenance of HSC quiescence. Other differentially regulated transcripts included genes known to be involved in self-renewal of HSCs (*Hlf* and *Meis1*) or to have roles in differentiation, the ubiquitin pathway, cell adhesion, chromatin modification, and various signaling pathways, including the MAPK pathway, which has been implicated in HSC maintenance (Ito et al., 2006). Thus, the transcriptional changes suggest that multiple stem cell-maintenance mechanisms are perturbed in the absence of Pbx1.

The lack of long-term self-renewal but preserved reconstitution potential, as well as increased proliferation, suggested that phenotypically defined *Pbx1*-deficient LT-HSCs display functional features of ST-HSCs and/or MPPs. To test this hypothesis, the *Pbx1* mutant LT-HSC gene set was interrogated for genes whose expression normally distinguishes LT- from ST-HSCs. To generate the latter gene set, LT- and ST-HSCs were prospectively sorted from the BM of WT mice and their global gene expression profiles were determined by microarray (Figure 6C). Bioinformatic analysis revealed a gene set of 2468 nonredundant transcripts that were differentially expressed between normal LT- and ST-HSCs subpopulations (Table S3), a higher number than previously reported by using different sorting and analysis strategies (Forsberg et al., 2005; Zhong et al., 2005). This gene set (LT- versus ST-HSCs) was then compared with the Pbx1-dependent LT-HSCs gene set. Among the transcripts downregulated in mutant LT-HSCs, 17% were also downregulated in normal ST-HSCs compared to LT-HSCs. Furthermore, among the transcripts upregulated in mutant LT-HSCs, a substantial proportion (37%) was also upregulated in normal ST-HSCs. Thus, many of the genes aberrantly expressed in phenotypically defined LT-HSCs from *Pbx1* mutant mice are normally expressed in ST-HSCs, but not WT LT-HSCs. The mutant LT-HSC gene signature was also compared with a previously published gene set differentially expressed in MPPs versus LT-HSCs (Kiel et al., 2005). A considerable overlap was observed between *Pbx1* mutant LT-HSC and normal MPP gene expression profiles (Figure 6D), further confirming that, in the absence of Pbx1, LT-HSCs prematurely express a transcriptional subprogram shared with downstream ST-HSCs and MPPs.

The functional and expression profiling studies suggested that Pbx1 regulates stem cell quiescence and exit from the LT self-renewing compartment. To further test this hypothesis, Gene Set Enrichment Analysis (GSEA) was employed to compare the Pbx1-regulated dataset with curated gene sets derived from diverse published experiments (Subramanian et al., 2005). To query the curated gene sets, the Pbx1-regulated dataset was reduced to a rank-ordered list of genes expressed by mutant versus WT LT-HSCs (more than 9684 nonredundant transcripts). In accordance with our hypothesis, GSEA revealed a strong correlation of genes downregulated in the absence of Pbx1 with gene sets that identify HSCs (Table 1 and Figure 6E). Conversely, the genes upregulated in the absence of Pbx1 strongly correlated with gene sets typical of progenitors (Table 1 and Figure 6E), as well as with cell-cycle-related gene sets. GSEA also revealed enrichment for Myc-activated genes and for genes involved in DNA damage control, possibly related to the perturbed cell-cycle status of *Pbx1* mutant LT-HSCs. Of note, genes downregulated in the absence of Pbx1 were also enriched for B cell gene sets, indicating that the CLPs and B cell abnormalities observed in mutant mice most likely originated from a LT-HSC defect in lymphoid priming.

Absence of Pbx1 Alters the Transcriptional Response to TGF-β in LT-HSCs

GSEA also confirmed a prominent perturbation of the TGF-β pathway in *Pbx1* mutant LT-HSCs as evidenced by significant enrichment of gene sets associated with TGF-β pathway alterations in various cell types (Table 1), including human cord blood CD34^{+} cells exposed to TGF-β in vitro (Figure 6E). Therefore, the integrity of the TGF-β signaling pathway was interrogated in prospectively purified mutant and WT LT-HSCs by assessing their transcriptional responses to TGF-β stimulation in vitro. In contrast to WT LT-HSCs, mutant LT-HSCs did not upregulate expression of several downstream transcripts in response to TGF-β stimulation (Figure 6F), including *Smad7*, *Klf4*, and *Ski*, as well as *Cdkn1c* (p57), recently implicated as an important

(E) Enrichment plots of selected gene sets from the GSEA in Table 1.
(F) Histogram shows fold induction for the indicated transcripts in sorted LT-HSCs upon 4 hr of TGF-β exposure, as measured by qRT-PCR (**$p < 0.0001$, *$p \leq 0.01$; p57: n = 7 mutants and 8 controls; *Smad7*: n = 3; *Klf4*, *Ski*: n = 4 mutants and 2 controls; *Ccnd2*, *Ccna2*: n = 4 and 3 mutants, respectively, and one control).

Table 1. Gene Sets with Strong Correlation to Genes Downregulated and Upregulated in the Absence of Pbx1

Gene Set Name	FDR	Gene Set Description
Downregulated Genes		
HSC Gene Sets		
HSC_LTHSC_FETAL	0.16	Upregulated in mouse LT-HSCs from fetal liver (FL)
HSC_LTHSC_SHARED	0.16	Upregulated in mouse LT-HSCs from both adult BM and FL
HSC_LTHSC_ADULT	0.18	Upregulated in mouse LT-HSCs from adult BM
HSC_HSCANDPROG_FETAL	0.18	Upregulated in mouse HSCs and progenitors from FL
FETAL_LIV_ENRICHED_TF	0.18	Transcription factors enriched in human fetal liver
HSC_HSCANDPROG_ADULT	0.18	Upregulated in mouse HSCs and progenitors from adult BM
HEMATOP_STEM_ALL_UP	0.22	Upregulated in human HSCs ($CD34^+/CD38^-/Lin^-$) versus $CD34^+/CD38^+/Lin^+$
ROSSI_AGING_UP	0.00	Upregulated in LT-HSCs from aging mice (= higher self-renewal) (Rossi et al., 2005)
FICARA_LTHSC_UP	0.00	Upregulated in WT LT-HSCs versus ST-HSCs (this study)
KIEL_LTHSC_UP	0.04	Upregulated in WT LT-HSCs versus MPP (Kiel et al., 2005)
TGF-β Gene Sets		
EMT_DN	0.17	Downregulated in the TGF-β-induced epithelial-to-mesenchymal transition
TGF_BETA_SIGNALING_PATH	0.18	Genes in the TGF-β signaling pathway
RUTELLA_HGHSNDCS_UP	0.22	Genes upregulated by HGF treatments (monocyte to TGF-β-producing DC)
SCANDURA_TGFBCD34_UP	0.00	Upregulated in hCB $CD34^+$ cells treated with TGF-β (Scandura et al., 2004)
B Cells Gene Sets		
HADDAD_CD45CD7_PvsM_DN	0.00	Genes enriched in $CD45RA^{int}CD7^-$ versus $CD45RA^{hi}CD7^{hi}$ HPCs
HADDAD_HSC_CD7_DN	0.00	Upregulated in human hHSCs of the line $CD45RA^{int}CD7^-$ versus $CD45RA^{hi}CD7^+$
HADDAD_HSC_CD10_UP	0.18	Upregulated in hHSC $CD45RA^{hi}Lin^-CD10^+$ versus $CD45RA^{int}CD7^-$ and $CD45RA^{hi}CD7^+$
HOFFMAN_BIVSBII_LGBII	0.23	Genes with 5-fold change in expression between large and small Pre-BII
HADDAD_HPCLYMPHO_ENRIC	0.22	Enriched in $CD45RA^{hi}Lin^-CD10^+$ versus $CD45RA^{int}CD7^-$ and $CD45RA^{hi}CD7^{hi}$
SIG_PIP3_SIGNALING_IN_B_L	0.23	Genes related to PIP3 signaling in B lymphocytes (SignalingAlliance)
C/EBP Gene Sets		
GERY_CEBP_TARGETS	0.05	Complete list of differentially regulated C/EBP-target genes
TAVOR_CEBP_UP	0.23	C/EBP upregulated genes in KCL22 cells
Upregulated Genes		
Cell-Cycle Gene Sets		
SERUM_FIBROBL_CELLCYCLE	0.00	Cell-cycle-dependent genes regulated after exposure to serum
CROONQUIST_IL6_STARV_UP	0.00	Upregulated in multiple myeloma cells exposed to IL-6
DNA_REPLICATION_REACT	0.00	http://www.genmapp.org
GOLDRATH_CELLCYCLE	0.00	Cell-cycle genes induced during antigen activation of $CD8^+$ T cells
CELL_CYCLE	0.00	Progression of events that occur during replication (GO)
CELL_CYCLE_KEGG	0.00	http://www.genmapp.org
BRENTANI_CELL CYCLE	0.00	Cancer-related genes involved in the cell cycle (Broad Institute)
CELL_CYCLE_CHECKPOINT	0.00	Point where progress through the cycle can be halted (GO)
G2PATHWAY	0.02	Biocarta
G1toS_ CELL_CYCLE_REACT	0.02	http://www.genmapp.org
Myc Gene Sets		
YU_CMYC_UP	0.00	Myc-activated genes
COLLER_MYC_UP	0.01	Genes upregulated by MYC in 293T
SCHUMACHER_MYC_UP	0.01	Genes upregulated by MYC in P493-6
ZELLER_MYC_UP	0.05	Genes upregulated by MYC in >3 papers
MYC_TARGETS	0.09	Myc-responsive genes reported in multiple systems
ST-HSC/Progenitors Gene Sets		
HSC_LATEPROG_FETAL	0.01	Upregulated in mouse hematopoietic late progenitors from FL
HSC_LATEPROG_ADULT	0.01	Upregulated in mouse hematopoietic late progenitors from adult BM
HSC_LATEPROG_SHARED	0.01	Upregulated in mouse hematopoietic late progenitors from both adult BM and FL
HSC_INTERMPROG_FETAL	0.19	Upregulated in mouse hematopoietic intermediate progenitors from FL

Table 1. *Continued*

Gene Set Name	FDR	Gene Set Description
Downregulated Genes		
HSC_INTERMPROG_SHARED	0.21	Upregulated in mouse hematopoietic intermed progenitors from adult BM and FL
FICARA_STHSC_UP	0.00	Upregulated in WT ST-HSCs versus LT-HSCs (this study)
ID1_KO_UP	0.00	Upregulated in Id1-KO mice (= progenitor phenotype) (Jankovic et al., 2007)
ROSSI_AGING_DOWN	0.01	Upregulated in LT-HSCs from young mice (= lower self-renewal)
Ubiquitin Pathway		
PROTEASOMEPATHWAY	0.10	www.broad.mit.edu/gsea/msigdb/cards/PROTEASOMEPATHWAY.html
PROTEASOMEDEGRADATION	0.19	Curated by Broad Institute
DNA Damage Control		
ATMPATHWAY	0.03	The protein kinase ATM responds to radiation-induced DNA damage
FERRANDO_MLL_T_ALL_DN	0.03	Cancer-related genes involved in DNA repair
DNA_DAMAGE_SIGNALING	0.07	Genes involved in DNA damage signaling (Broad Institute)
UVB_SCC_UP	0.14	Upregulated by UV-B light in squamous cell carcinoma cells
ROTH_HTERT_DIFF	0.24	Involved in DNA repair and cell-cycle control in hTERT-transduced cells

Gene sets in italic do not belong to the GSEA data set; they have been curated by F.F. et al.

regulator of HSC quiescence (Scandura et al., 2004; Umemoto et al., 2005; Yamazaki et al., 2006). Furthermore, unlike control LT-HSCs, *Ccnd2* and *Ccna2* were not downregulated by TGF-β simulation in mutant LT-HSCs, consistent with their in vivo cycling activity. These results together with the global transcriptional changes suggest that Pbx1 controls stem cell quiescence and self-renewal at least in part by affecting the response to TGF-β.

DISCUSSION

In this study, we demonstrate that the *Pbx1* proto-oncogene and global developmental regulator serves a critical role within the hematopoietic system to support the self-renewal of adult HSCs as one of few known factors involved in maintaining their quiescence. Transcriptional profiling suggests that multiple stem cell maintenance programs are perturbed in the absence of Pbx1, including genes associated with the response to TGF-β signaling. This suggests potential mechanisms for facilitating loss of quiescence, inappropriate cell-cycle entry, and initiation of a transcriptional program resembling that of more mature multipotent progenitors. As a consequence, LT-HSCs lose their major defining characteristic, i.e., self-renewal, and progressively exhaust themselves in the absence of Pbx1.

Among the multiple stem cell maintenance factors that are altered in Pbx1-deficient LT-HSCs, a significant proportion are linked with the TGF-β pathway, which is increasingly implicated in regulation of HSC quiescence. TGF-β has recently been suggested as a possible BM niche signal necessary to induce LT-HSC "hibernation" through inhibition of lipid raft clustering in response to cytokine stimulation (Yamazaki et al., 2007). The CDKI p57 appears to be responsible for regulating this quiescent HSC state (Yamazaki et al., 2007). Consistent with these observations, cell-cycle arrest of human cord blood $CD34^+$ cells in response to TGF-β requires p57 (Scandura et al., 2004). Moreover, p57 is responsible for cell-cycle arrest of mouse KSL side population (SP) cells (Umemoto et al., 2005), suggesting that it is one of the main contributors to maintenance of LT-HSC quiescence. We observed higher expression levels of *Cdkn1c* in LT-HSCs compared to ST-HSCs (although the difference did not meet our stringent statistical requirements for inclusion in Table S3). This is consistent with previous studies performed with different methods and mouse strains showing that *Cdkn1c* is preferentially expressed in LT-HSCs compared to ST-HSCs and MPPs (Kiel et al., 2005) and at higher baseline levels in mouse $CD34^-$ KSL cells (highly enriched for LT-HSCs) than other CDKIs such as *p21* or *p27* (Yamazaki et al., 2006). Although the latter are also implicated in HSC or progenitor self-renewal, we did not observe their expression levels to be altered in *Pbx1*-deficient LT-HSCs in contrast to the marked reduction in *p57*.

In support of a possible role for Pbx1 on a pathway that regulates the balance between stem cell quiescence/hibernation and cell-cycle entry, the *Cdkn1c* gene was not induced by TGF-β stimulation of prospectively isolated *Pbx1* mutant LT-HSCs. Although these data do not rule out a secondary role for *Cdkn1c*, it is one of very few in our Pbx1-dependent gene set to contain a Pbx1 heterodimer binding site in proximity to its promoter. Furthermore, Pbx1/Prep transcriptional complexes have been shown to interact with Smads (Bailey et al., 2004), the nuclear effectors of TGF-β signaling, and Pbx1 transcriptional complexes regulate expression of the *p21* gene in a myelomonocytic cell line (Bromleigh and Freedman, 2000). In epithelial cells, a FoxO/Smad complex is implicated in TGF-β upregulation of *p15ink4a*, another CDKI (Gomis et al., 2006). Thus, there are precedents for regulation of CDKI genes by Pbx and/or Smad proteins. However, perturbed expression of Smad7, a TGF-β pathway regulator that has been implicated in HSC self-renewal (Blank et al., 2006), was also observed in *Pbx1*-deficient HSCs in vitro and in vivo, raising the possibility of a more global compromise of the response to TGF-β. Because our data were obtained 4 weeks after *Pbx1* deletion, it is theoretically possible that they reflect in part compensatory changes in the proliferation activity or differentiation state of the stem cell compartment. Further investigations are necessary to establish a causal relationship between the hematopoietic defects caused by Pbx1 loss and perturbed regulation of TGF-β pathway-associated genes implicated in HSC self-renewal.

HSC reductions associated with the absence of Pbx1 were only apparent from ~3 weeks postbirth despite the fact that expression of the *Tie2Cre* transgene initiates in definitive HSCs with their emergence in the aorta-gonad-mesonephros and yolk sac during embryonic development. The postnatal onset of the Pbx1 phenotype likely reflects differences in the proliferation states of embryonic/fetal and adult BM HSCs. During development, HSCs undergo massive expansion while preserving their self-renewal capacity, whereas HSCs in the postnatal BM are mostly quiescent starting from 3–4 weeks of age (Bowie et al., 2006), and their ability to maintain quiescence correlates with the maintenance of self-renewal and engraftment potential (Passegue et al., 2005). Thus, onset of the *Pbx1*-deficient HSC phenotype in *Tie2Cre.Pbx1* mice correlates with the postnatal requirement for HSC quiescence for maintenance of self-renewal.

A role for Pbx1 in maintaining stem cell quiescence significantly broadens its contributions beyond previous studies, which have consistently implicated it in promoting progenitor cell expansion during development of multiple organs (Brendolan et al., 2005; Kim et al., 2002; Manley et al., 2004; Selleri et al., 2001), including the hematopoietic system (DiMartino et al., 2001). Thus, Pbx1 appears to have divergent but functionally complementary roles in the maintenance of HSC quiescence versus promotion of progenitor proliferation, and our current results raise the possibility that other Pbx1-deficient phenotypes may in part reflect its impact on tissue-specific stem cells. The potential complexity of its contributions in the hematopoietic progenitor compartment was suggested by earlier studies demonstrating that HoxB4-mediated HSC in vitro expansion is further enhanced by concurrent reduction of *Pbx1* expression (Krosl et al., 2003), which appeared inconsistent with its role in promoting progenitor expansion. However, a major function for Pbx1 in maintaining LT-HSC quiescence provides a likely explanation for its antagonistic effects because HoxB4 overexpression enhances HSC expansion without affecting long-term self-renewal potential. The divergent roles for Pbx1 in HSCs versus progenitors may reflect possible context-dependent contributions to the expression of CDKI and other cell-cycle regulatory genes.

In addition to a stem cell defect, a marked reduction was observed in the BM pro- and pre-B cell compartments, as well as a striking reduction in CLPs, suggesting a role for Pbx1 at a critical stage of lymphoid development where acute leukemia likely originates and confirming previous results from our laboratory obtained with a different experimental approach (Sanyal et al., 2007). The extremely low number of CLPs in mutant mice prevented studies of their cell-cycle status, although the cycling rates of pro- and pre-B cells were only mildly decreased (data not shown), consistent with previous conclusions that Pbx1 may be dispensable from the pro-B stage onward (Sanyal et al., 2007). The striking CLP hypoplasia may reflect a cell-intrinsic requirement for Pbx1 in CLPs or alternatively be the consequence of insufficient CLP generation due to an aberrant differentiation program initiated by *Pbx1* null HSCs. In support of the latter, GSEA revealed a defect in lymphoid priming present at the LT-HSC stage. The expression of lymphoid-specific genes in LT-HSCs and the concept of lineage priming in stem cells have been previously reported (Mansson et al., 2007; Rossi et al., 2005). In *Pbx1*-deficient mice, the lymphoid priming defect does not completely compromise further differentiation capacity, because mature B cells are present in BM, spleen, and PB of primary KO mice and transplant recipients. In future studies, it will be of interest to further characterize the roles of Pbx1 in HSC lymphoid priming and generation of CLPs and the potential relevance of these contributions for Pbx1 oncoproteins in B cell precursor leukemias.

EXPERIMENTAL PROCEDURES

Mice

Transgenic *Tie2Cre*, *Mx1Cre*, and $Pbx1^{+/-}$ mice have been described (Chang et al., 2004; Kisanuki et al., 2001; Kuhn et al., 1995; Selleri et al., 2001). These strains were intercrossed to generate $Tie2Cre^{+}.Pbx1^{+/-}$ or $MxCre^{+}.Pbx1^{+/-}$ mice, which were subsequently bred with $Pbx1^{f/f}$ mice (to be described elsewhere) to obtain $Tie2Cre^{+}.Pbx1^{-/f}$, $MxCre^{+}.Pbx1^{-/f}$, or $MxCre^{+}.Pbx1^{f/f}$ mutants and their littermate controls, fully or partially backcrossed onto a C57BL/6 background. Mutant and control mice were genotyped by PCR. $Tie2Cre^{+}.Pbx1^{-/f}$ were viable but displayed a short life span and died of unknown causes between 3 and 7 weeks of age. Congenic Ly5.1 mice, purchased from Jackson Laboratories (Bar Harbor, ME), were maintained in the Stanford animal facility and used as recipients of BM transplantation experiments. Congenic C57BL/6 Ly5.2 mice were crossed with Ly5.1 mice to obtain Ly5.1/Ly5.2 competitor BM cells. All experiments were performed with the approval of and in accordance with Stanford's Administrative Panel on Laboratory Animal Care.

Histology

Tissues were fixed in 10% (weight/volume) formalin, embedded in paraffin, sectioned, and stained with hematoxylin and eosin.

Flow Cytometry

BM cell suspensions were obtained by flushing of femurs and tibiae in sterile staining buffer (see below). PB was obtained by tail bleeding. Staining of cells for FACS analysis was performed in deficient RPMI (Irvine Scientific) containing 3% fetal calf serum, 1 mM EDTA, and 0.01 M HEPES (staining buffer) with the following conjugated monoclonal antibodies (mAbs) obtained from either BD PharMingen (BD) or eBioscience (San Diego, CA): Mac1/CD11b (M1/70), B220 (RA3-6B2), CD43 (S7), IgM^{b} (AF6-78), TCRβ (H57-597), NK1.1 (PK136), TER119 (TER-119), c-Kit (2B8), Sca1 (D7 or E13-161.7), IL-7Rα (SB14), CD16/32 (2.4G3), CD34 (RAM34), CD48 (HM48-1), CD41 (MWReg30), Ly5.1 (A20), Ly5.2 (104), and CD135 (AF2 10.1). The lineage cocktail included the following Cy7PE-conjugated mAbs: Mac1, Gr1 (RB6-8C5), B220, TER119, CD3 (145-2C12), CD4 (GK1.5), and CD8 (53-6.7). CD150 (TC15-12F12.2) was purchased from BioLegend. Stained cells were analyzed with an LSR1A flow cytometer or FACSAria (BD Biosciences, San Jose, CA). Cell sorts were performed with a FACSVantage (BD Biosciences). Cell Quest Pro or Diva software (BD) and FlowJo (Tree Star) were used for data acquisition and analysis, respectively. For Annexin V staining, freshly isolated BM cells were first stained with the appropriate mAbs, then washed in binding buffer and incubated with Annexin V FITC (BD).

Cell-Cycle Analysis

Mice received a single intraperitoneal injection of 5-bromodeoxyuridine (BrdU) 2 hr prior to sacrifice. In order to have enough cells for the analysis of LT-HSCs, BM cells were obtained by the crushing of multiple bones (femurs, tibia, humerous, ulna, shoulder blades, sternum, and spine). Progenitors were purified based on the expression of c-Kit by using anti-CD117 magnetic microbeads and an automated cell separator (AutoMACS, Miltenyi Biotec, Auburn, CA) and then subjected to cell surface staining for detection of stem cells. Analysis of BrdU incorporation was performed with the FITC BrdU Flow Kit (BD PharMingen) according to the manufacturer's protocol. For H/PY staining, purified $c\text{-}Kit^{+}$ cells were incubated with cell surface markers to detect HSCs and then incubated with HOECHST 33342 (Invitrogen) and Pyronin Y (Sigma-Aldrich) as previously described (Passegue et al., 2005).

Transplantation Assays

Transplantation of BM cells from mutant or control mice (with or without 2 × 10^5 competitor BM cells), or secondary transplantation of donor-derived BM cells from primary recipients, was performed by retro-orbital injection of lethally irradiated Ly5.1 mice (900 cGy). For secondary transplants, three doses of sorted Ly5.2 cells were injected: 1 × 10^6, 5 × 10^5, and 2 × 10^5 (three mice/group). Data from the three different doses were pooled because the outcome did not correlate with the number of injected cells.

5-FU Treatment

Two-week-old *MxCre*$^+$.*Pbx1*$^{f/f}$ (or $^{-/f}$) or control mice received poly(I:C) injections (InvivoGen, San Diego, CA) every other day for a total of seven injections. Five weeks after the last injection, mice received 150 mg/kg 5-FU (ICN Pharmaceuticals, Inc., Costa Mesa, CA) i.p. at 7 day intervals.

Colony-Forming Unit Assays

BM cells (2 × 10^4) were seeded into methylcellulose-containing medium (methoCult 3234; Stem Cell Technologies) in the presence of SCF (20 ng/ml), IL-6, IL-3 (10 ng/ml each), and Epo (3 U/ml). Colonies were counted after 10 days of culture.

Statistical Analysis

The significance of differences was determined by two-tailed Student's t test.

Microarray and Bioinformatics Analyses

Two-week-old *MxCre*$^+$.*Pbx1*$^{f/f}$ or *MxCre*$^-$.*Pbx1*$^{f/f}$ mice were given seven poly(I:C) injections every other day and sacrificed 4 weeks after the last injection. BM cells were obtained from multiple bones of individual mice, immunomagnetically selected for c-Kit expression, then stained with conjugated mAbs (CD34, CD135, Sca-1, lineage cocktail, and c-Kit) prior to sorting. Cells were maintained on ice when possible through all procedures. RNA from sorted cell populations (3–5000 LT-HSCs, 4–12,000 ST-HSCs) was purified with Trizol and subjected to two rounds of amplification with a Two-Cycle Target Labeling and Control Reagent (Affymetrix, Santa Clara). Microarray experiments were performed in the Stanford PAN Facility with Affymetrix 430-2.0 arrays. Arrays were scanned with a Gene Chip Scanner 3000 (Affymetrix) running GCOS 1.1.1 software. Scanned data were exported to dChip software for normalization, statistical analysis, and heat mapping. A perfect-match/mismatch (PM/MM) model was used for the calculation of expression values (Li and Wong, 2001). The threshold for considering genes differentially expressed was 1.3-fold difference with a 90% confidence. Raw data are available for download from Gene Expression Omnibus (http://ncbi.nlm.nih.gov/geo). The categorization of genes into functional groupings was based on the Gene Ontology (GO) classification system as well as on comprehensive evaluation of the relevant literature for all of the differentially regulated genes. Gene set enrichment analysis (Subramanian et al., 2005) was performed with GSEA v2.0 software available from the Broad Institute (http://www.broad.mit.edu/gsea).

Real-Time Quantitative PCR

For studies of TGF-β-dependent transcriptional response, LT-HSCs were sorted from poly(I:C)-treated *MxCre*$^+$*Pbx1*$^{f/f}$ or control mice as described for the microarray experiments and then incubated for 4 hr in StemPro-34SFM medium (GIBCO) with 2 ng/ml TGF-β1 (PeproTech, Rocky Hill, NJ) prior to RNA extraction with a PicoPure RNA Isolation Kit (Arcturus, Mountain View, CA) and amplification with a RiboAmp RNA Amplification Kit (Arcturus). cDNA was prepared with Superscript First-Strand Synthesis System for RT-PCR (Invitrogen, Carlsbad, CA) and then subjected to real-time PCR with TaqMan probes (Applied Biosystems, Foster City, CA).

SUPPLEMENTAL DATA

Supplemental Data include four figures and three tables and can be found with this article online at http://www.cellstemcell.com/cgi/content/full/2/5/484/DC1/.

ACKNOWLEDGMENTS

We thank Maria Ambrus and Cita Nicolas for technical assistance and Tim C. Somervaille for critically reading the manuscript. F.F. was supported by a fellowship from the American-Italian Cancer Foundation and an ASH Fellow Scholar Award in basic research. We acknowledge support from PHS grants CA42971 and CA90735.

Received: September 28, 2007
Revised: February 19, 2008
Accepted: March 11, 2008
Published: May 7, 2008

REFERENCES

Akala, O.O., and Clarke, M.F. (2006). Hematopoietic stem cell self-renewal. Curr. Opin. Genet. Dev. *16*, 496–501.

Bailey, J.S., Rave-Harel, N., McGillivray, S.M., Coss, D., and Mellon, P.L. (2004). Activin regulation of the follicle-stimulating hormone beta-subunit gene involves Smads and the TALE homeodomain proteins Pbx1 and Prep1. Mol. Endocrinol. *18*, 1158–1170.

Berkes, C.A., Bergstrom, D.A., Penn, B.H., Seaver, K.J., Knoepfler, P.S., and Tapscott, S.J. (2004). Pbx marks genes for activation by MyoD indicating a role for a homeodomain protein in establishing myogenic potential. Mol. Cell *14*, 465–477.

Blank, U., Karlsson, G., Moody, J.L., Utsugisawa, T., Magnusson, M., Singbrant, S., Larsson, J., and Karlsson, S. (2006). Smad7 promotes self-renewal of hematopoietic stem cells. Blood *108*, 4246–4254.

Bowie, M.B., McKnight, K.D., Kent, D.G., McCaffrey, L., Hoodless, P.A., and Eaves, C.J. (2006). Hematopoietic stem cells proliferate until after birth and show a reversible phase-specific engraftment defect. J. Clin. Invest. *116*, 2808–2816.

Brendolan, A., Ferretti, E., Salsi, V., Moses, K., Quaggin, S., Blasi, F., Cleary, M.L., and Selleri, L. (2005). A Pbx1-dependent genetic and transcriptional network regulates spleen ontogeny. Development *132*, 3113–3126.

Bromleigh, V.C., and Freedman, L.P. (2000). p21 is a transcriptional target of HOXA10 in differentiating myelomonocytic cells. Genes Dev. *14*, 2581–2586.

Cellot, S., and Sauvageau, G. (2007). Zfx: at the crossroads of survival and self-renewal. Cell *129*, 239–241.

Chang, C.P., Neilson, J.R., Bayle, J.H., Gestwicki, J.E., Kuo, A., Stankunas, K., Graef, I.A., and Crabtree, G.R. (2004). A field of myocardial-endocardial NFAT signaling underlies heart valve morphogenesis. Cell *118*, 649–663.

Cheng, T., Rodrigues, N., Shen, H., Yang, Y., Dombkowski, D., Sykes, M., and Scadden, D.T. (2000). Hematopoietic stem cell quiescence maintained by p21cip1/waf1. Science *287*, 1804–1808.

DiMartino, J.F., Selleri, L., Traver, D., Firpo, M.T., Rhee, J., Warnke, R., O'Gorman, S., Weissman, I.L., and Cleary, M.L. (2001). The Hox cofactor and proto-oncogene Pbx1 is required for maintenance of definitive hematopoiesis in the fetal liver. Blood *98*, 618–626.

Forsberg, E.C., Prohaska, S.S., Katzman, S., Heffner, G.C., Stuart, J.M., and Weissman, I.L. (2005). Differential expression of novel potential regulators in hematopoietic stem cells. PLoS Genet *1*, e28. 10.1371/journal.pgen.0010028.

Galan-Caridad, J.M., Harel, S., Arenzana, T.L., Hou, Z.E., Doetsch, F.K., Mirny, L.A., and Reizis, B. (2007). Zfx controls the self-renewal of embryonic and hematopoietic stem cells. Cell *129*, 345–357.

Gomis, R.R., Alarcon, C., Nadal, C., Van Poznak, C., and Massague, J. (2006). C/EBPbeta at the core of the TGFbeta cytostatic response and its evasion in metastatic breast cancer cells. Cancer Cell *10*, 203–214.

Ito, K., Hirao, A., Arai, F., Takubo, K., Matsuoka, S., Miyamoto, K., Ohmura, M., Naka, K., Hosokawa, K., Ikeda, Y., and Suda, T. (2006). Reactive oxygen species act through p38 MAPK to limit the lifespan of hematopoietic stem cells. Nat. Med. *12*, 446–451.

Jankovic, V., Ciarrocchi, A., Boccuni, P., DeBlasio, T., Benezra, R., and Nimer, S.D. (2007). Id1 restrains myeloid commitment, maintaining the self-renewal

capacity of hematopoietic stem cells. Proc. Natl. Acad. Sci. USA *104*, 1260–1265.

Kamminga, L.M., Bystrykh, L.V., de Boer, A., Houwer, S., Douma, J., Weersing, E., Dontje, B., and de Haan, G. (2006). The Polycomb group gene Ezh2 prevents hematopoietic stem cell exhaustion. Blood *107*, 2170–2179.

Kiel, M.J., Yilmaz, O.H., Iwashita, T., Terhorst, C., and Morrison, S.J. (2005). SLAM family receptors distinguish hematopoietic stem and progenitor cells and reveal endothelial niches for stem cells. Cell *121*, 1109–1121.

Kim, S.K., Selleri, L., Lee, J.S., Zhang, A.Y., Gu, X., Jacobs, Y., and Cleary, M.L. (2002). Pbx1 inactivation disrupts pancreas development and in Ipf1-deficient mice promotes diabetes mellitus. Nat. Genet. *30*, 430–435.

Kisanuki, Y.Y., Hammer, R.E., Miyazaki, J., Williams, S.C., Richardson, J.A., and Yanagisawa, M. (2001). Tie2-Cre transgenic mice: a new model for endothelial cell-lineage analysis in vivo. Dev. Biol. *230*, 230–242.

Kondo, M., Weissman, I.L., and Akashi, K. (1997). Identification of clonogenic common lymphoid progenitors in mouse bone marrow. Cell *91*, 661–672.

Krosl, J., Beslu, N., Mayotte, N., Humphries, R.K., and Sauvageau, G. (2003). The competitive nature of HOXB4-transduced HSC is limited by PBX1: the generation of ultra-competitive stem cells retaining full differentiation potential. Immunity *18*, 561–571.

Kuhn, R., Schwenk, F., Aguet, M., and Rajewsky, K. (1995). Inducible gene targeting in mice. Science *269*, 1427–1429.

Li, C., and Wong, W.H. (2001). Model-based analysis of oligonucleotide arrays: expression index computation and outlier detection. Proc. Natl. Acad. Sci. USA *98*, 31–36.

Manley, N.R., Selleri, L., Brendolan, A., Gordon, J., and Cleary, M.L. (2004). Abnormalities of caudal pharyngeal pouch development in Pbx1 knockout mice mimic loss of Hox3 paralogs. Dev. Biol. *276*, 301–312.

Mansson, R., Hultquist, A., Luc, S., Yang, L., Anderson, K., Kharazi, S., Al-Hashmi, S., Liuba, K., Thoren, L., Adolfsson, J., et al. (2007). Molecular evidence for hierarchical transcriptional lineage priming in fetal and adult stem cells and multipotent progenitors. Immunity *26*, 407–419.

Moens, C.B., and Selleri, L. (2006). Hox cofactors in vertebrate development. Dev. Biol. *291*, 193–206.

Passegue, E., Wagers, A.J., Giuriato, S., Anderson, W.C., and Weissman, I.L. (2005). Global analysis of proliferation and cell cycle gene expression in the regulation of hematopoietic stem and progenitor cell fates. J. Exp. Med. *202*, 1599–1611.

Rossi, D.J., Bryder, D., Zahn, J.M., Ahlenius, H., Sonu, R., Wagers, A.J., and Weissman, I.L. (2005). Cell intrinsic alterations underlie hematopoietic stem cell aging. Proc. Natl. Acad. Sci. USA *102*, 9194–9199.

Saleh, M., Rambaldi, I., Yang, X.J., and Featherstone, M.S. (2000). Cell signaling switches HOX-PBX complexes from repressors to activators of transcription mediated by histone deacetylases and histone acetyltransferases. Mol. Cell. Biol. *20*, 8623–8633.

Sanyal, M., Tung, J.W., Karsunky, H., Zeng, H., Selleri, L., Weissman, I.L., Herzenberg, L.A., and Cleary, M.L. (2007). B-cell development fails in the absence of the Pbx1 proto-oncogene. Blood *109*, 4191–4199.

Scandura, J.M., Boccuni, P., Massague, J., and Nimer, S.D. (2004). Transforming growth factor beta-induced cell cycle arrest of human hematopoietic cells requires p57KIP2 up-regulation. Proc. Natl. Acad. Sci. USA *101*, 15231–15236.

Schnabel, C.A., Godin, R.E., and Cleary, M.L. (2003a). Pbx1 regulates nephrogenesis and ureteric branching in the developing kidney. Dev. Biol. *254*, 262–276.

Schnabel, C.A., Selleri, L., and Cleary, M.L. (2003b). Pbx1 is essential for adrenal development and urogenital differentiation. Genesis *37*, 123–130.

Selleri, L., Depew, M.J., Jacobs, Y., Chanda, S.K., Tsang, K.Y., Cheah, K.S., Rubenstein, J.L., O'Gorman, S., and Cleary, M.L. (2001). Requirement for Pbx1 in skeletal patterning and programming chondrocyte proliferation and differentiation. Development *128*, 3543–3557.

Subramanian, A., Tamayo, P., Mootha, V.K., Mukherjee, S., Ebert, B.L., Gillette, M.A., Paulovich, A., Pomeroy, S.L., Golub, T.R., Lander, E.S., and Mesirov, J.P. (2005). Gene set enrichment analysis: a knowledge-based approach for interpreting genome-wide expression profiles. Proc. Natl. Acad. Sci. USA *102*, 15545–15550.

Tothova, Z., Kollipara, R., Huntly, B.J., Lee, B.H., Castrillon, D.H., Cullen, D.E., McDowell, E.P., Lazo-Kallanian, S., Williams, I.R., Sears, C., et al. (2007). FoxOs are critical mediators of hematopoietic stem cell resistance to physiologic oxidative stress. Cell *128*, 325–339.

Umemoto, T., Yamato, M., Nishida, K., Yang, J., Tano, Y., and Okano, T. (2005). p57Kip2 is expressed in quiescent mouse bone marrow side population cells. Biochem. Biophys. Res. Commun. *337*, 14–21.

Venezia, T.A., Merchant, A.A., Ramos, C.A., Whitehouse, N.L., Young, A.S., Shaw, C.A., and Goodell, M.A. (2004). Molecular signatures of proliferation and quiescence in hematopoietic stem cells. PLoS Biol. *2*, e301. 10.1371/journal.pbio.0020301.

Yamazaki, S., Iwama, A., Takayanagi, S., Morita, Y., Eto, K., Ema, H., and Nakauchi, H. (2006). Cytokine signals modulated via lipid rafts mimic niche signals and induce hibernation in hematopoietic stem cells. EMBO J. *25*, 3515–3523.

Yamazaki, S., Iwama, A., Morita, Y., Eto, K., Ema, H., and Nakauchi, H. (2007). Cytokine signaling, lipid raft clustering, and HSC hibernation. Ann. N Y Acad. Sci. *1106*, 54–63.

Zhong, J.F., Zhao, Y., Sutton, S., Su, A., Zhan, Y., Zhu, L., Yan, C., Gallaher, T., Johnston, P.B., Anderson, W.F., and Cooke, M.P. (2005). Gene expression profile of murine long-term reconstituting vs. short-term reconstituting hematopoietic stem cells. Proc. Natl. Acad. Sci. USA *102*, 2448–2453.